PAPER

Direct current microhollow cathode discharges on silicon devices operating in argon and helium

IOP Publishing Plasma Sources Science and Technology
Plasma Sources Sci. Technol. 27 (2018) 025005 (10pp) https://doi.org/10.1088/1361-6595/aaa870

Direct current microhollow cathode discharges on silicon devices operating in argon and helium

R Michaud[1], V Felix[1], A Stolz[1], O Aubry[1], P Lefaucheux[1], S Dzikowski[2], V Schulz-von der Gathen[2], L J Overzet[3] and R Dussart[1,4]

[1] GREMI, Univ. Orleans—CNRS, 14 rue d'Issoudun, BP 6744, F-45067, Orléans, France
[2] Experimental Physics II, Ruhr-Universität Bochum, D-44780, Bochum, Germany
[3] PSAL, University of Texas at Dallas, Richardson, TX 75080-3021, United States of America

E-mail: remi.dussart@univ-orleans.fr

Received 31 October 2017, revised 11 January 2018
Accepted for publication 17 January 2018
Published 6 February 2018

Abstract

Microhollow cathode discharges have been produced on silicon platforms using processes usually used for MEMS fabrication. Microreactors consist of 100 or 150 μm-diameter cavities made from Ni and SiO_2 film layers deposited on a silicon substrate. They were studied in the direct current operating mode in two different geometries: planar and cavity configuration. Currents in the order of 1 mA could be injected in microdischarges operating in different gases such as argon and helium at a working pressure between 130 and 1000 mbar. When silicon was used as a cathode, the microdischarge operation was very unstable in both geometry configurations. Strong current spikes were produced and the microreactor lifetime was quite short. We evidenced the fast formation of blisters at the silicon surface which are responsible for the production of these high current pulses. EDX analysis showed that these blisters are filled with argon and indicate that an implantation mechanism is at the origin of this surface modification. Reversing the polarity of the microdischarge makes the discharge operate stably without current spikes, but the discharge appearance is quite different from the one obtained in direct polarity with the silicon cathode. By coating the silicon cathode with a 500 nm-thick nickel layer, the microdischarge becomes very stable with a much longer lifetime. No current spikes are observed and the cathode surface remains quite smooth compared to the one obtained without coating. Finally, arrays of 76 and 576 microdischarges were successfully ignited and studied in argon. At a working pressure of 130 mbar, all microdischarges are simultaneously ignited whereas they ignite one by one at higher pressure.

Supplementary material for this article is available online

Keywords: MHCD, microplasma, microdischarge, silicon, instability

1. Introduction to DC microdischarges on silicon

Direct current micro hollow cathode discharges (MHCD) were first introduced in the mid 90s by Schoenbach *et al* [1]. An MHCD consists of a dielectric plate sandwiched between two planar electrodes, which are drilled, at least partially, forming a sub-millimeter hole. Due to their small dimension and their large surface to volume ratio, the produced microplasma remains cold and can stably operate at atmospheric pressure in the normal regime provided that the cathode area is not fully utilized [2, 3].

The denomination for MHCD was initially given because a steep increase in voltage at low current was followed by a negative slope and then a plateau at higher current. The negative slope of the voltage as a function of current was attributed to a classical hollow cathode effect [2, 4]. However, Boeuf *et al* showed that this voltage decrease was actually

[4] Author to whom any correspondence should be addressed.

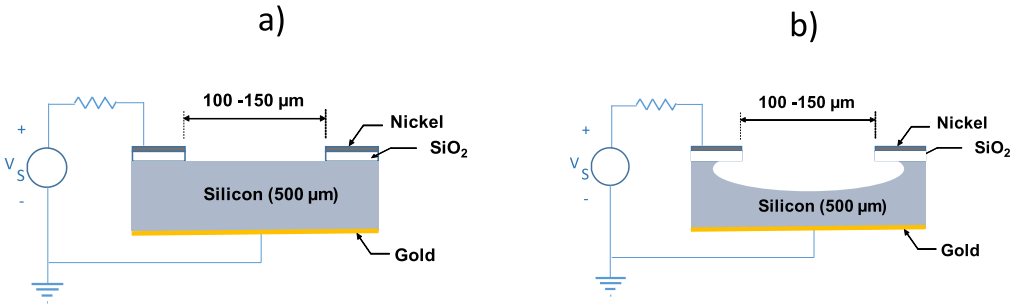

Figure 1. Schematics of the microdischarge reactors. (a) Planar configuration. (b) Isotropically etched cavity configuration.

due to a transition of the discharge from the abnormal regime for which the plasma was located inside the hollow cathode to a normal glow discharge where much of the current was drawn through the outer surface of the cathode [5]. Indeed, using very thin electrodes, such a voltage drop is not observed because the discharge directly develops to the normal glow on the outer surface of the cathode [3]. Boeuf *et al* also showed that pendulum electrons were not responsible for the particular shape of the *I–V* characteristics because the electron energy-loss mean free path was too short to allow electrons emitted from one part of the cathode to reach the opposite sheath with enough energy to ionize [5]. The denomination 'MHCD' for such a structure was maintained anyway, even if no clear micro hollow cathode effect was evidenced.

Although the breakdown follows remarkably well a Paschen curve with a minimum of the breakdown voltage at around 1 Torr cm [6], the discharge can be ignited by field effect as studied and reviewed by Go *et al* [7] and reported by other teams [8]. However, this effect becomes dominant for very short interelectrode distances, typically below 5 μm at atmospheric pressure.

Microdischarges on silicon were introduced shortly after MHCDs by Eden's team [9]. Intensively developed silicon processing for microelectronic and MEMS devices offers many new opportunities to design accurate, original and efficient devices to produce high density microplasmas. Eden *et al* first used 200–400 μm-diameter cavities made from metallurgical grade silicon as a cathode of DC discharges. They were operating at 130 Torr in neon, nitrogen or air [9]. Then, they introduced a new geometry obtained by wet etching forming inverted pyramids from the (111) planes of silicon [10]. Again, silicon was used as a cathode. The dielectric consisted of a 8 μm-thick polyimide layer, which was covered by a thin nickel film for the anode. Typical currents below 1 μA were driven through each microcavity in Ne. The authors reported that the device was becoming unstable by reversing the polarity. The lifetime of the device was limited to few hours and the failure was attributed to the thinness of the nickel layer. Park *et al* also demonstrated the photosensitivity of their devices when using p-type silicon and showed that the sensitivity was much higher than what is obtained using Si avalanche photodiode [11]. Finally, they reported on the microdischarges operation in DC with cross sections of $(10\ \mu m)^2$ or $(30\ \mu m)^2$ and a depth of 200 μm in a mixture of Xe and O_2 [12]. Then, they mainly focused on MHCDs working in a DBD mode with an additional dielectric layer between the two electrodes and excited by a high frequency (kHz) alternative current [13–15].

Silicon microdischarge devices operating in DC with currents of the order of 1 mA per cavity were studied by several other teams [16–18]. Even if arrays containing 1024 microplasmas were successfully ignited, the device operation is unstable and produces many current spikes that significantly damage the microcavities and lead to device failure. The mechanism responsible for this unstable operation and short lifetime was investigated in [19]. In this paper, we discuss different possibilities to enhance the stability of microdischarges made from silicon wafers, limit the damage and increase their lifetime for currents above 1 mA.

2. Microreactors and experimental setup

The two different microreactors geometries used in this experiment are schematically represented in the figure 1. The planar geometry (figure 1(a)) consists of a flat silicon surface covered partially by a 8 μm-thick SiO_2 layer and a 1 μm-thick nickel layer. The so-called 'cavity geometry' is similar to the previous one except that the silicon is isotropically etched to a typical depth of 30 μm. Pictures of four microdevices containing either a single cavity or an array of 39 cavities are shown in figures 2(a) and (b), respectively. The diameter of the cavity is 100 or 150 μm. The backside of the wafer is covered by a thin film of gold to produce a good ohmic contact. More than 15 individual process steps including cleaning, oxidation, lithography, deposition and etching are necessary to create such a structure.

A ballast resistor between 1 kΩ and 1 MΩ is connected to the front side of the device to limit the current. The microdischarges are then connected to a high-precision, high-voltage DC power supply (Heinzinger—1500 V maximum voltage, 100 mA maximum current). A very low frequency between 10 and 100 mHz triangle signal was applied to the power supply to control the linear increase and decrease of the high-voltage applied to the microdevice. Discharge voltage and current were measured by two high voltage probes (Tektronix P5100) placed before and after the ballast resistance and monitored on an oscilloscope (Tektronix TDS 3014B, 100 MHz). *V–I* characteristics are directly obtained by a LabVIEW program taking into account the internal resistances of the probes. For current

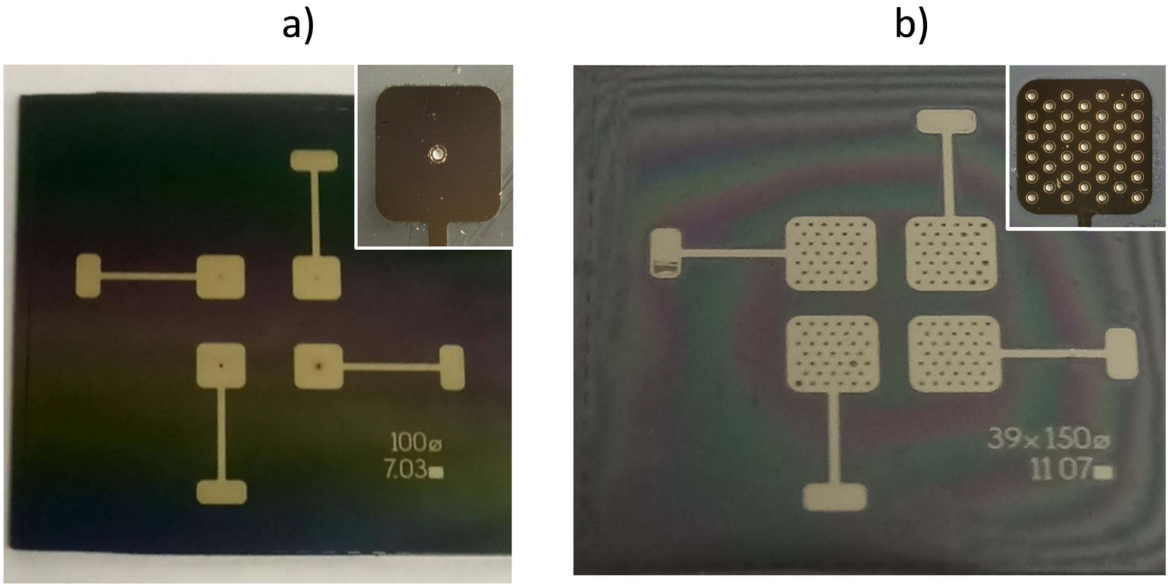

Figure 2. Examples of microdischarge devices. Insets: zoom in of one of the four microreactor for each configuration. (a) 100 μm-diameter single hole samples. (b) Arrays of 39 microcavities having a diameter of 150 μm.

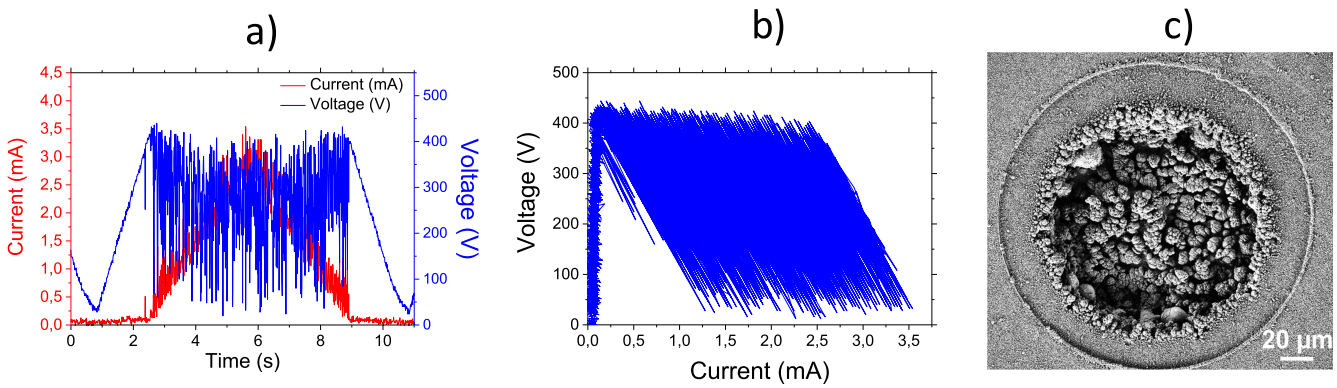

Figure 3. Results with a single 150 μm diameter planar silicon cathode sample operating in Ar at atmospheric pressure. (a) Voltage and current versus time. (b) *V–I* characteristic. (c) SEM top view of the surface after about 1 min of plasma operation.

spike analysis, an inductive current probe (Tektronix CT-1, 1 GHz) was placed between the back side and the ground. The chamber is evacuated to a base pressure of the order of 10^{-5} mbar and filled with the desired gas (Ar or He in these experiments) three times to reduce the contamination by air. The microdischarges were monitored using a high-speed microscope (Keyence VW-9000) equipped with a long-distance zoom unit (macrozoom unit VW-72 or high performance zoom lens VH-750W). The surface of the microdevice was observed and analyzed after operation using a Zeiss SUPRA40 scanning electron microscope (SEM) coupled with an energy-dispersive x-ray spectroscopy (EDS) analysis system (Bruker QUANTAX).

3. Mechanisms of instabilities obtained with silicon cathodes

An example of the discharge current and voltage time evolution obtained with argon at atmospheric pressure is shown in figure 3(a). A single 150 μm diameter microreactor with a planar configuration was used. First, the voltage is linearly increased up to 415 V until breakdown occurs. Then, the current is increased and reaches a maximum of about 3 mA after 5 s (100 mHz frequency for the triangle signal). But the discharge is very unstable: a multitude of current and voltage spikes are produced immediately after the discharge is ignited. In figure 3(b), the resulting *V–I* characteristic is shown with oscillations of the *V–I* curve following a slope corresponding to the ballast resistor (here 300 kΩ). For a lower ballast resistor, much higher intensity current peaks can be produced where typical values in the order of 1 A for current spikes could be obtained [19]. After plasma operation of about 1 min (about 6 signal periods), the device was destroyed. A SEM top view of the reactor surface after failure is shown in figure 3(c). The larger circle corresponds to the boundary between the remaining resist and the nickel surface. The surface affected by the discharge appears very rough with some micrometric cauliflower structures formed on the cathode and at the edge of the anode. The same degradation of the

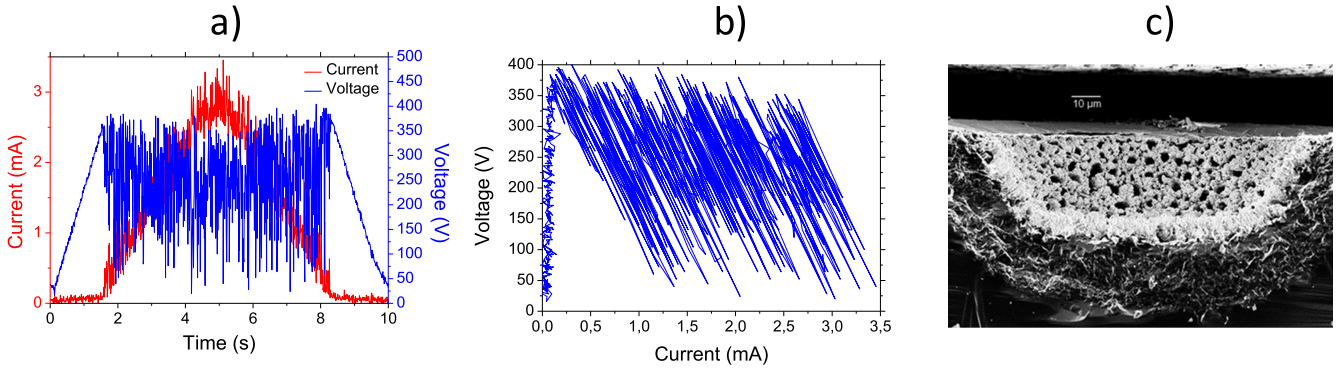

Figure 4. Results with a single 100 μm diameter cavity silicon cathode sample operating in Ar at atmospheric pressure. (a) Voltage and current versus time. (b) *V–I* characteristic. (c) SEM cross-section view of the surface after about 2 min of plasma operation.

cathode surface was reported by several groups using silicon as a cathode even in cavity geometry configuration [16–18]. As described by Lindner *et al* [17], some experiments in silicon microhollow cathode operating in DC are described and show the same type of cathode erosion with a very rough surface after operation. In [18], experiments for gas conversion of chemical contaminants were performed in silicon microreactors operating in neon in DC or in a pulsed regime. Even if the surface is a little bit less eroded in the pulsed regime, in both regimes, the resulting surface after plasma looks very similar to the surface shown in figure 3(c). This erosion limits dramatically the lifetime of the devices because, as explained in [16, 18], some melted silicon and/or nickel is redeposited in the interelectrode space leading to a short circuit. Using a cavity geometry, the same instability behavior is observed. However, the lifetime is longer in this cavity configuration. Indeed, with the interelectrode distance being larger in that configuration, it takes more time to cover the dielectric surface between the two electrodes before creating a short circuit. Voltage and current versus time with the corresponding *V–I* characteristics as well as a SEM cross section view of the micro device after 2 min of operation are shown in figures 4(a)–(c), respectively. The average voltage and current evolutions are very close to those obtained in the planar configuration. The surface damage is also very similar: a very porous structure is produced at the surface.

In order to get a better understanding of the mechanism, some characterization after the first minutes of plasma operation was carried out. First, using the high-speed camera, small bright (10 μm diameter) spots appearing simultaneously with the high current spikes were evidenced [19]. Such an intensive spot is shown in figure 5(a) where an array of 16 microplasmas having a cavity geometry with a diameter of 150 μm was ignited in helium at 350 mbar. SEM observation was carried out after only 30 s of operation at a current as low as 125 μA (figure 5(b)). Even at this low current value, some degradation of the cathode surface occurs. As shown in [19], some blisters of different size are formed. They appear clearly in the figure 5(b) where 5–10 μm-large blisters can be observed. The rest of a popped blister can also be identified. This effect was attributed to an implantation mechanism [19]. Note that such blisters are also obtained in argon microplasma. The explosion of a blister is followed by a bright spot and a high current spike which correspond to the generation of a constricted microplasma [19]. To investigate the content of these blisters, EDS was carried out on a silicon cathode after a plasma of few seconds, before the explosion of the first blisters. A SEM view of the surface is shown in figure 6(a). As observed, most of the blisters formed at the surface have not yet exploded. EDS measurements were carried out at two positions for comparison: one on a not yet popped blister and one on a popped blister (crosses shown on figure 6(b), which is a zoom of figure 6(a)). The EDS spectrum of each location is given in figure 6(c). It reveals that blisters are composed of silicon, oxygen and argon whereas the exploded blister is mainly composed of silicon and oxygen, but in a smaller proportion. This EDS analysis confirms the implantation mechanism of argon ions at the very near surface of the silicon or silicon dioxide.

Note that the distribution of the blisters shown in figure 6(a) is quite uniform at the surface of the cavity in this planar cathode configuration whereas it was shown in [19] that larger blisters were obtained at the edge of the cavity aperture. Indeed, in the case of a cavity configuration like the one used in figure 5(a) and in [19], the electric field is maximum at the edge of the aperture where the distance between the two electrodes is shorter. In the planar configuration, the electric field is more uniform on the cathode surface leading to a more uniform distribution of the blisters.

We suggest the following mechanism to explain the formation of micro arc from blisters. As observed by EDS analysis (figure 6), an SiO_x layer is formed at the surface of the blister. Inside the blisters that are not yet popped, argon is trapped due to ion implantation, which is at the origin of the blister formation. Since a thin SiO_x dielectric layer is obtained at the surface of the blister, we can deduce that positive charges can accumulate on this surface. Then, a high voltage can be obtained between the silicon cathode and the top edge of the blister where positive charges accumulate. This can cause a constricted discharge, which is evidenced by observed high current spikes and transient bright spots.

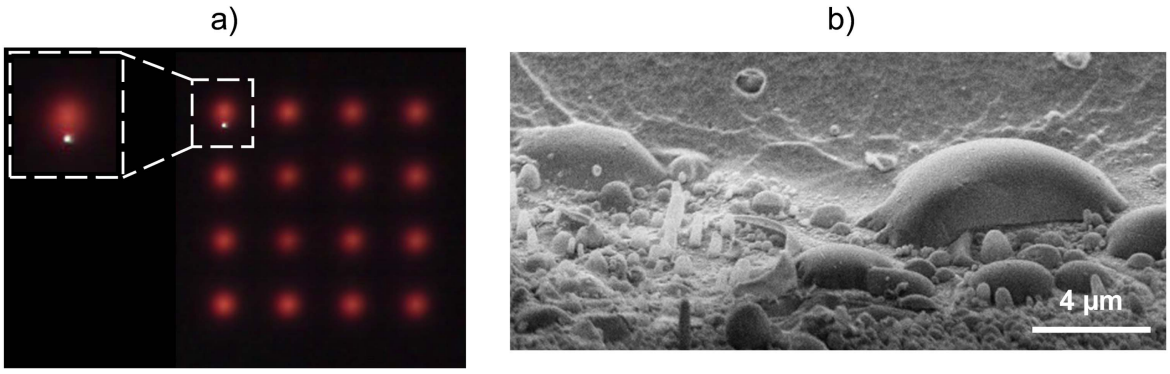

Figure 5. (a) Array of 16 microdischarges with a diameter of 150 μm operating in He at 350 mbar. Evidence of a bright spot appearance at the edge of one of the microplasmas. (b) Surface of the silicon microcathode observed by SEM after 30 s of operation in He at 350 mbar mbar with a current of 125 μA.

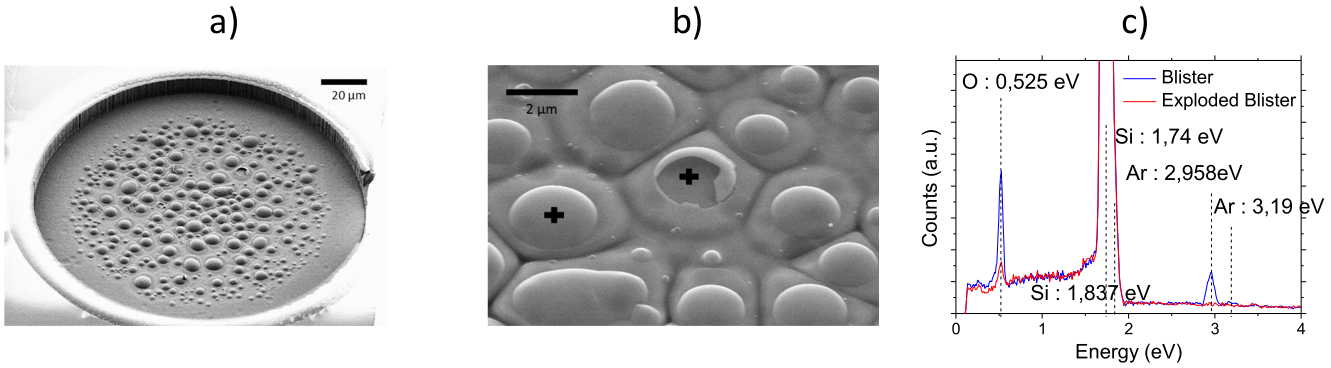

Figure 6. Results with a single 150 μm diameter planar silicon cathode sample operating in Ar at atmospheric pressure after 20 s of operation. (a) SEM picture of the microreactor. (b) SEM picture of the blisters (crosses correspond to the targeted locations for EDX measurements). (c) EDX measurements for one blister (in blue) and for one exploded blister (in red).

4. Ways to reduce or avoid instabilities and enhance the microdischarge lifetime

Silicon remains a relevant material in order to integrate microdischarges and some electronic circuits nearby on a same chip. However, for application perspectives, the lifetime of the microdevice has to be enhanced significantly. Different ways have been investigated to make microdischarges much more stable, without creating blisters and high current spikes. As reported in [19], the addition of about 1% of SF_6 to helium increases the lifetime of the microreactor by reducing the arc occurrence. It also avoids the formation of blisters by etching the surface from the reaction of fluorine with silicon. However, this solution is not quite satisfactory since it requires an undesired gas and modifies the cavity dimensions during the operation of the microdischarge. In the next sub-sections, two other ways are investigated to avoid instabilities and high current spikes.

4.1. Reversed polarity

The microdischarge bias can be reversed to avoid the implantation of the ions in silicon, which is now used as an anode. The experiment was performed on a planar configuration with a 150 μm-diameter single microdischarge. Voltage and current versus time are shown in figure 7(a) for a microdischarge in Ar (200 mbar) operating in reverse polarity. The corresponding *V–I* curve is given in figure 7(b). As observed on the two figures, Ar discharge in such polarity conditions is very stable: no current spike is observed. The discharge follows a normal regime because the plasma can freely expand on the nickel cathode large area when the current is raised. An image of the discharge is shown in figure 7(c). As observed, for this experiment, a nickel ring shape pattern was used as a cathode. Interestingly, a bright spot having a diameter of approximately 40 μm appears in the center of the 150 μm diameter anode. This bright spot is only obtained at a pressure between 130 and 500 mbar. At higher pressures, a bright ring shape at the edge of the anode appears instead (see inset of figure 8(a)). At pressures below 130 mbar, the microdischarge does not ignite, but a macroscopic plasma can form with another grounded surface inside the chamber so that no light emission is observed from the anode area (see inset of the figure 8(c)). This effect is attributed to the sheath typical dimension that changes with pressure. A schematic of the three different cases is represented in figure 8. Beyond 500 mbar, the sheath remains quite thin (thickness of the order of the dielectric one [6]) and follows the cathode shape (figure 8(a)). The bright area appears annular because electrons reaching the anode concentrate on a ring. This behavior has already been observed and reported in AC operating mode [20]. Between 100 and

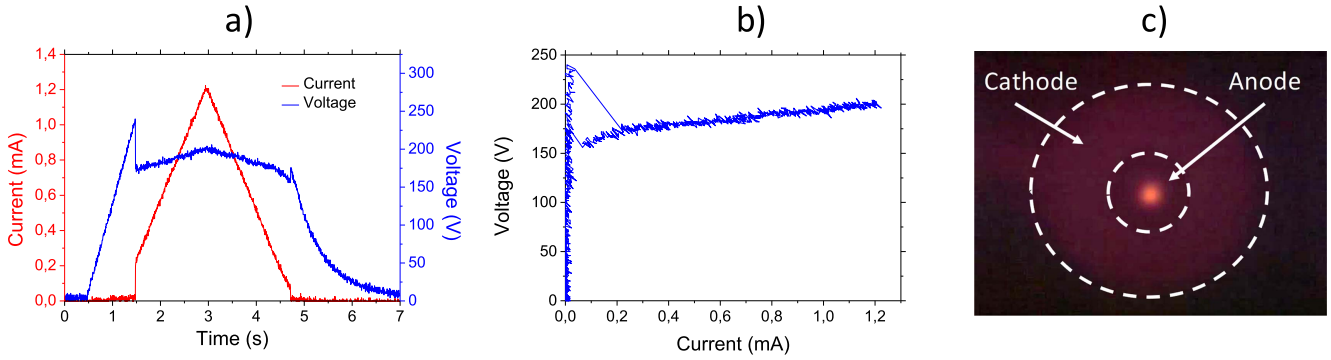

Figure 7. Results with a single 150 μm diameter planar silicon cathode sample operating in Ar at 200 mbar in reversed polarity. (a) Voltage and current versus time. (b) *V–I* characteristic. (c) Camera picture of the microplasma.

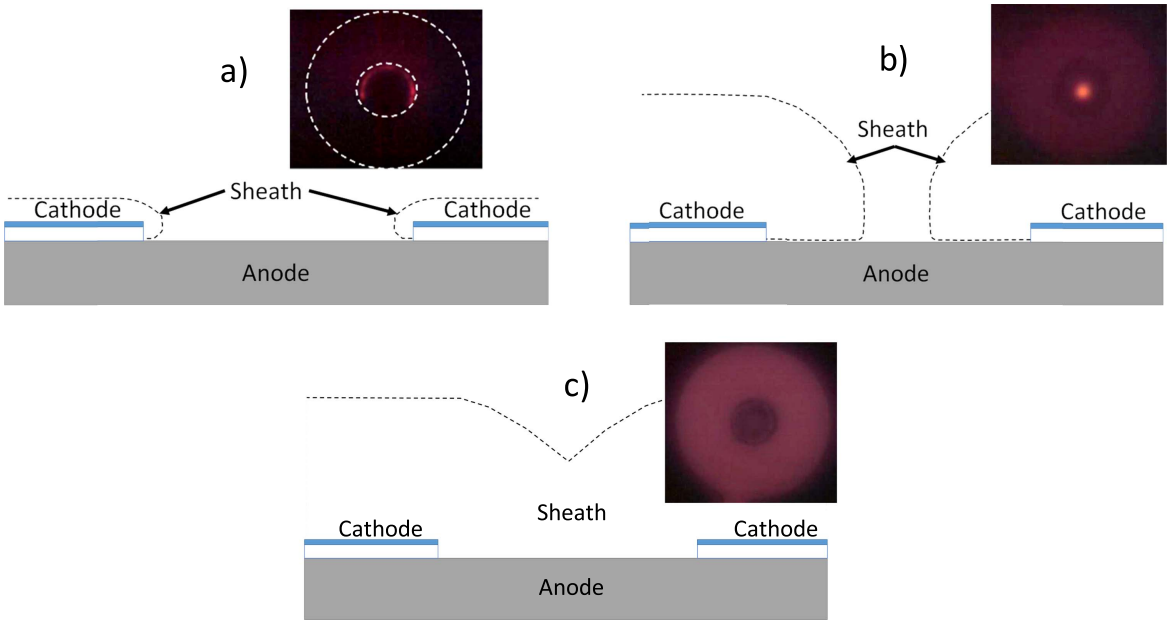

Figure 8. Schematic of the sheath as function of pressure. (a) Pressure beyond 500 mbar. Inset: camera picture of a 1 bar Ar microplasma. (b) Pressure between 100 and 500 mbar. Inset: camera picture of a 350 mbar Ar microplasma. (c) Pressure below 100 mbar. Inset: camera picture of a 100 mbar Ar microplasma.

500 mbar, a spot appears at the center of the hole (inset of figure 8(b)). Electrons are confined by the sheath boundary and follow a path that concentrate them on this spot zone. Below 100 mbar, the anode is totally covered by the sheath (figure 8(c)). Hence, only a macroscopic discharge can be obtained between the cathode and another grounded area of the chamber. In this reversed polarity configuration, the microdischarge has a long lifetime and is stable over the time but is not confined inside the hole.

4.2. Nickel coating

As mentioned and explained in the previous parts, silicon is not a suitable cathode material for DC microdischarge. However, it has been shown in the previous paragraph that no current spike was appearing when using the microdischarge in reversed polarity: the discharge is actually very stable in this polarity conditions. This suggests that nickel seems to be a more appropriate material than silicon for the microdischarge cathode. To check it, the flat silicon cathode surface was coated by a 400 nm-thick nickel layer (figure 9(a)). In figure 9(b), different *V–I* curves from argon microdischarges in direct polarity obtained with a 1 MΩ ballast resistance are shown for different pressures. As observed, for 130 and 400 mbar, no instability occurred during the operation and an abnormal regime (discharge voltage increases with current) is obtained because the discharge rapidly covers the entire cathode area. At 670 and 1000 mbar, an instability in the *V–I* characteristic is observed at low current (below 0.28 mA for 1000 mbar), which corresponds to the self-pulsing regime already reported and explained by another team [21, 22]. At higher current, the discharge remains stable and follows a quasi-normal regime (quasi-constant discharge voltage) indicating that the cathode is not totally covered by the sheath, but only a part of the cathode provides secondary emission of electrons. To test the robustness of these microreactors having a nickel cathode, a higher maximum current was injected. Figure 10(a) shows voltage and current versus time for a

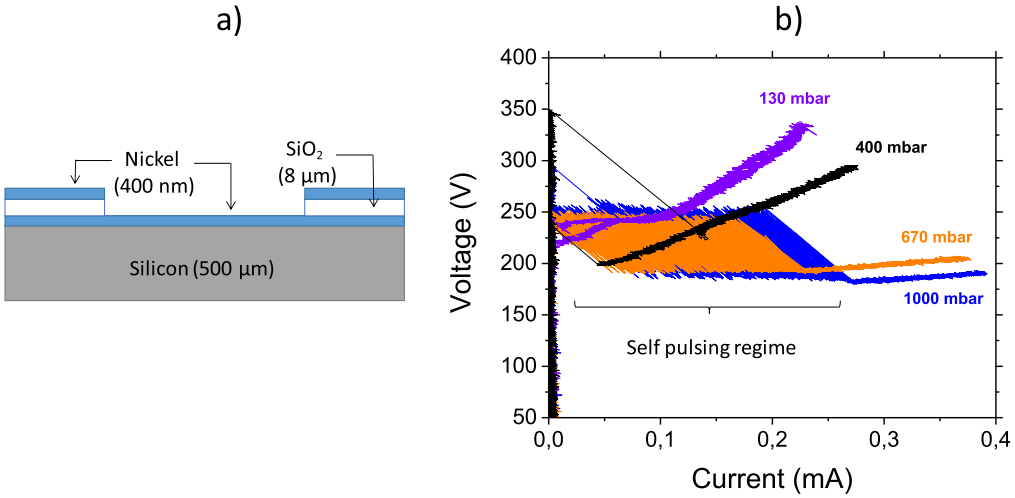

Figure 9. (a) Schematic of the microdischarge reactors with nickel electrodes. (b) *V–I* curves for a single 150 μm-diameter planar 400 nm-thick nickel sample operating in Ar at different pressures.

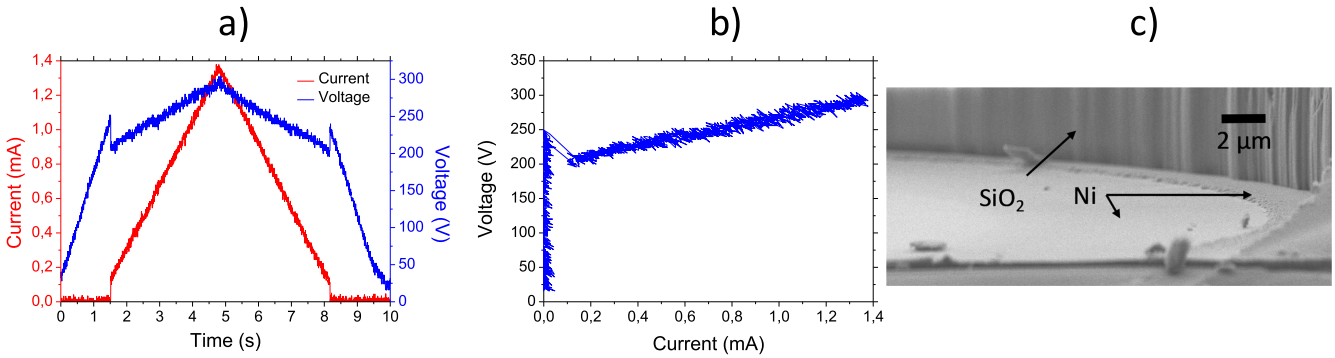

Figure 10. Results with a single 150 μm diameter planar 500 nm thick nickel sample operating in Ar at atmospheric pressure. (a) Voltage and current versus time. (b) *V–I* characteristic. (c) SEM picture of the cathode surface after few minutes of microplasma.

150 μm-diameter planar microdischarge with a nickel cathode surface operating in argon at atmospheric pressure. The maximum current is 1.4 mA. No instability was observed during the operation of the microdischarge. This behavior is stable over time and very reproducible. It also works stably in He gas. As observed in figure 10(b), the microdischarge follows an abnormal regime because the plasma is confined on the limited cathode surface area. After several minutes of operation, SEM views shown in figure 10(c) were recorded and no blisters at the nickel surface are exhibited. Nevertheless, we can observe an erosion effect by comparing the center of the cathode with the edge. This erosion is probably due to sputtering. Despite this erosion mechanism, nickel seems to be a very good candidate for the cathode material and definitely better than silicon. Indeed, in the case of nickel, no ion implantation is obtained between the oxide layer and the nickel, probably because nickel is less oxidized than silicon. Moreover, charges cannot accumulate at the surface of the nickel especially because nickel oxide is more conductive than SiO_2. In the next paragraph, a cavity geometry of the cathode was investigated in order to increase the injected power density and enhance the lifetime of the microreactor.

4.3. Operation with a cavity geometry coated by nickel

The cavity of an isotropically etched silicon hole corresponding to the figure 1(b) configuration was coated with a thin nickel layer of about 500 nm. In this case, two main differences compared to the planar configuration can be noticed: first, the interelectrode distance is about three times larger reducing the electric field before breakdown and the dielectric surface separating the two electrodes is also larger so that the total coating of this surface area by sputtered material takes more time, which delays a potential short circuit. Figure 11(a) shows the time evolution of voltage and current of a 100 μm-diameter microdischarge operating in argon in direct polarity at atmospheric pressure. The maximum value of the discharge current reaches 5 mA in these experimental conditions. The corresponding *V–I* characteristic is given in figure 11(b). As observed on the characteristic, the plasma can work stably during for several minutes. No current spike was obtained during the discharge operation even at this rather high current value. In this configuration, the discharge follows an abnormal regime between 2 and 5 mA (figure 11(b)). A SEM picture of a cavity profile after 5 min operation is shown in figure 11(c). If we compare this profile to the one obtained with silicon cathode (figure 4(c)), it is clear that nickel

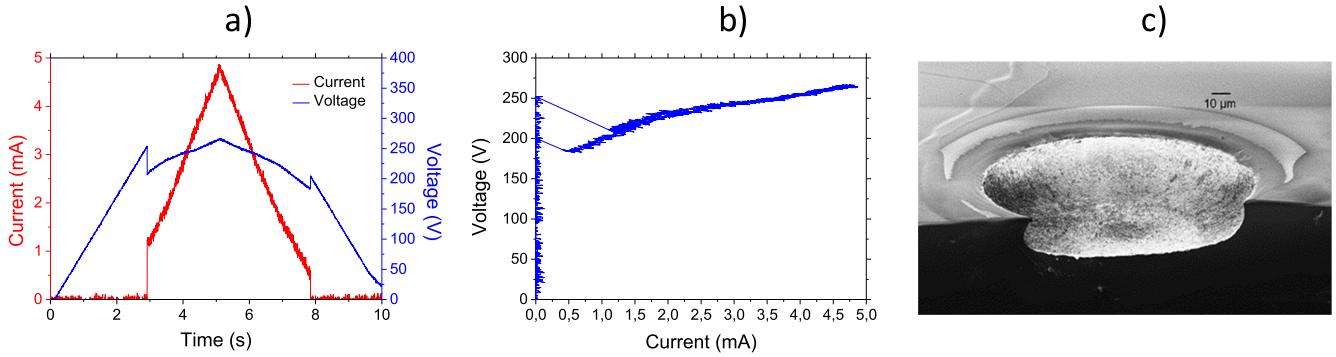

Figure 11. Results with a single 100 μm-diameter cavity nickel cathode sample operating in Ar at atmospheric pressure. (a) Voltage and current versus time. (b) *V–I* characteristic. (c) SEM picture of the surface after about 5 min of plasma operation.

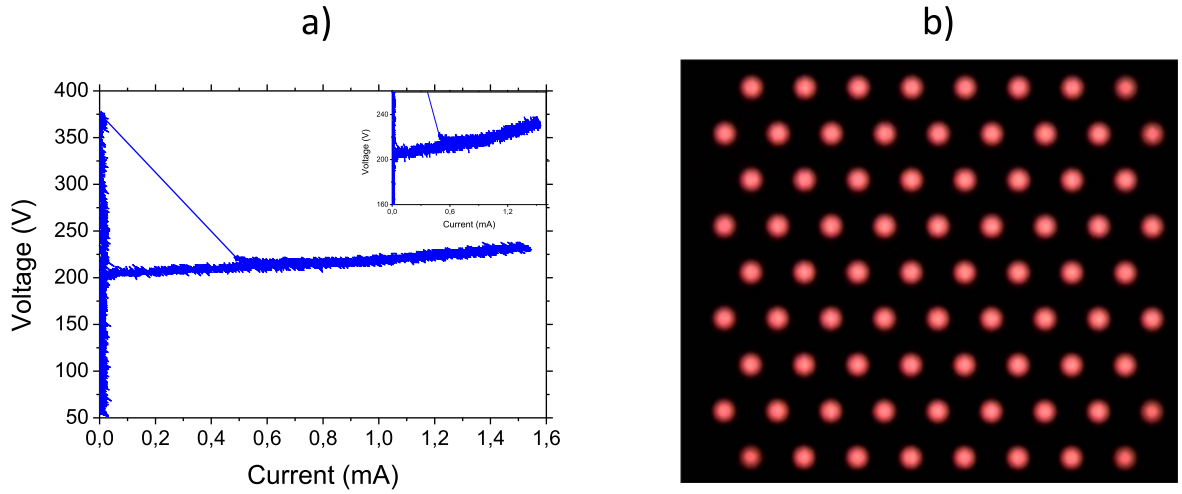

Figure 12. Array of 76 microdicharges having a diameter of 100 μm operating in 130 mbar of Ar. (a) *V–I* characteristic. Inset: zoom in of the *V–I* curve. (b) Picture of the microplasma array.

efficiently prevents cavity damage. No blisters are formed at the surface and the surface remains smooth compared to the very porous one obtained when using silicon.

5. Microdischarge arrays operating in DC

An array containing 76 microreactors in planar configuration with a nickel cathode was ignited. The hole diameter was 100 μm and the center-to-center distance between the holes was 300 μm. The *V–I* characteristic obtained in argon at 130 mbar is given figure 12(a). A picture of the microplasma array in operation is shown in figure 12(b). All the microdischarges of the array are lit with a total current of about 1.5 mA, which gives an average current of 20 μA per microdischarge. At 130 mbar, all microdischarges ignite simultaneously as observed in the movie provided online (stacks.iop.org/PSST/27/025005/mmedia) (Ar array at 130 mbar), which clearly shows the simultaneous ignition of the microdischarges when the voltage is linearly increased. At this scale, from the *V–I* curve, the discharge seems to follow a quasi-normal regime after breakdown. However, as observed in figure 9(a), in single microdischarge the discharge voltage increases more significantly at low pressure, and this is also shown by the inset of figure 12(a) where we zoomed in on the *Y* axis. At 260 mbar of argon, using the same array, the ignition is quite different: microdischarges ignite one by one, and preferentially next to a microdischarge that is already on (see movie Ar array at 260 mbar).

At pretty low pressure, a larger sheath is expected due to a lower electron density. Hence, one microdischarge can have a more significant influence on its neighbor and trigger the ignition almost instantaneously. This phenomenon was confirmed using another array containing up to 576 microreactors, but in cavity configuration this time, with a 100 μm-diameter and a center-to-center distance of 200 μm. The discharge was ignited in He gas. A picture of the array working at 130 mbar is given on figure 13(a). All the microdischarges are lit. The *V–I* characteristics obtained at 130 and 260 mbar are given in figures 13(b) and (c), respectively. The total current reaches more than 23 mA in this case, which gives an average current of 40 μA per microdischarge. As for the array in Ar, at 130 mbar, all the 576 microdischarges ignite simultaneously (see movie He array at 130 mbar, provided online). The *V–I* curve follows an abnormal regime as well. At 260 mbar, the array switches on following a kind of ignition wave from the center left side to the other sides (see movie He array at 260 mbar). The *V–I*

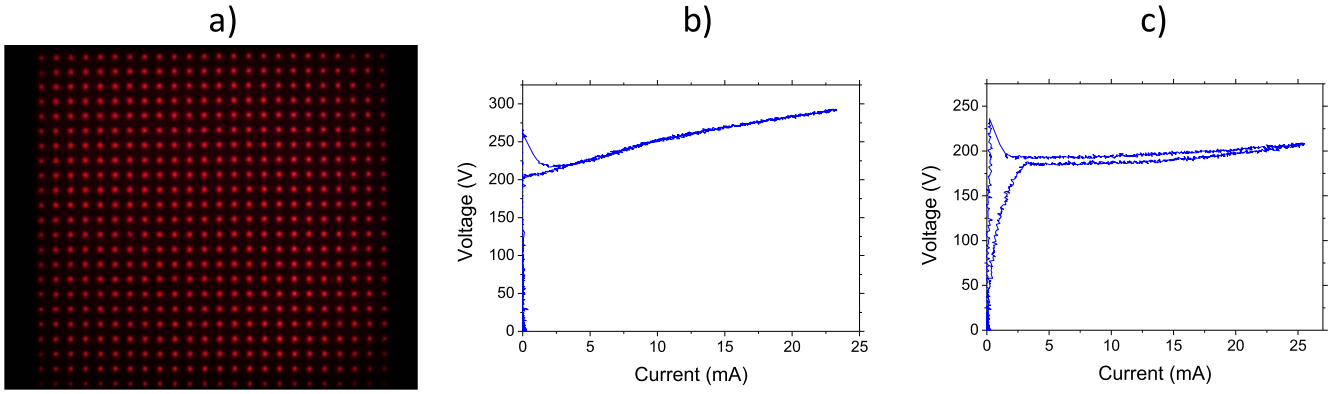

Figure 13. Array of 576 microdicharges having a diameter of 100 μm operating in He. (a) Picture of the microplasma array. (b) *V–I* characteristic at 130 mbar. (c) *V–I* characteristic at 260 mbar.

curve follows a normal regime (see figure 13(c)) before the array is entirely lit. In this case, indeed, before all microdischarges are ignited, the available cathode area is not fully covered by the plasma and the current density remains constant while the current is increased, which maintains the discharge voltage constant. At 260 mbar, a hysteresis effect is also observed on the *V–I* curve that is not obtained at 130 mbar. This hysteresis is attributed to a heating mechanism, especially obtained for higher electron and ion density. It was confirmed by experiments carried out at higher pressure and with arrays containing even more microreactors. The cathode surface heats up due to the ion bombardment and provides more electrons to the plasma and increases the plasma conductivity.

6. Conclusions

Microdischarge devices have been built on silicon wafer by microfabrication techniques and studied in DC operation in argon and helium for different cathode geometries and materials. Microdischarges using silicon as cathode material present many instabilities and are unstable. This behavior was attributed to the formation of blisters at the surface that appear after only few seconds of operation. After argon operation, EDS analysis was carried out on the cathode area and showed that these blisters were filled with argon. When a blister pops, a current spike appears and causes the degradation of the cathode surface. Melted silicon is redeposited by projection inside the cavity, which can cause some short circuit between the two electrodes. This effect reduces the lifetime of the microdevice. By reversing the polarity, it is possible to significantly enhance the microreactor lifetime. In this case, the discharge extends freely on the opened cathode area and a bright spot appears at the middle of the anode for intermediate pressures (200–500 mbar). As compared to the direct bias case, the microdischarge is less localized. Another solution to obtain stable and localized microdischarges consists in coating the silicon cathode surface with nickel. In this case, the discharge becomes very stable and the lifetime is much longer even at rather high currents (more than 1 mA). In the planar configuration, the limiting factor of the lifetime is the erosion of the nickel layer deposited on the silicon. By changing the geometry with a nickel coated silicon cavity, a higher current can be driven through the microdischarge. Arrays of hundreds of microreactors have been successfully ignited. At low pressure, typically less than 150 mbar, all microdischarges ignite simultaneously, whereas they ignite one by one at higher pressures. A hysteresis effect can be observed on the *V–I* characteristic of the 576 microdischarges array due to the heating of the sample.

Acknowledgments

This work was supported in part by the German Academic Exchange Service and the French Foreign Ministry through the PROCOPE Project grant 57134635 and was carried out within the framework of the CRC1316 of the German Research Foundation. The microdischarge devices were made within the CTU IEF-MINERVE facility which is partly supported by the RENATECH network.

ORCID iDs

R Michaud https://orcid.org/0000-0001-6432-052X
V Schulz-von der Gathen https://orcid.org/0000-0002-7182-3253
R Dussart https://orcid.org/0000-0003-2001-5034

References

[1] Schoenbach K H, Verhappen R, Tessnow T, Peterkin F E and Byszewski W W 1996 Microhollow cathode discharges *Appl. Phys. Lett.* **68** 13–5
[2] Schoenbach K H, Moselhy M, Shi W and Bentley R 2003 Microhollow cathode discharges *J. Vac. Sci. Technol.* A **21** 1260–5
[3] Dufour T, Dussart R, Lefaucheux P, Ranson P, Overzet L J, Mandra M, Lee J-B and Goeckner M 2008 Effect of limiting the cathode surface on direct current microhollow cathode discharge in helium *Appl. Phys. Lett.* **93** 71508

[4] Schoenbach K H, El-Habachi A, Shi W and Ciocca M 1997 High-pressure hollow cathode discharges *Plasma Sources Sci. Technol.* **6** 468–77
[5] Boeuf J P, Pitchford L C and Schoenbach K H 2005 Predicted properties of microhollow cathode discharges in xenon *Appl. Phys. Lett.* **86** 71501
[6] Dufour T, Overzet L J, Dussart R, Pitchford L C, Sadeghi N, Lefaucheux P, Kulsreshath M and Ranson P 2010 Experimental study and simulation of a micro-discharge with limited cathode area *Eur. Phys. J.* D **60** 565–74
[7] Go D B and Venkattraman A 2014 Microscale gas breakdown: ion-enhanced field emission and the modified Paschen's curve *J. Phys. D: Appl. Phys.* **47** 503001
[8] Klas M, Matejčík š, Radjenović B and Radmilović-Radjenović M 2011 Experimental and theoretical studies of the breakdown voltage characteristics at micrometre separations in air *Europhys. Lett.* **95** 35002
[9] Frame J W, Wheeler D J, DeTemple T A and Eden J G 1997 Microdischarge devices fabricated in silicon *Appl. Phys. Lett.* **71** 1165–7
[10] Park S-J, Chen J, Liu C and Eden J G 2001 Silicon microdischarge devices having inverted pyramidal cathodes: fabrication and performance of arrays *Appl. Phys. Lett.* **78** 419–21
[11] Park S-J, Eden J G and Ewing J J 2002 Photodetection in the visible, ultraviolet, and near-infrared with silicon microdischarge devices *Appl. Phys. Lett.* **81** 4529–31
[12] Park S-J, Eden J G, Chen J and Liu C 2004 Microdischarge devices with 10 or 30 μm square silicon cathode cavities: pd scaling and production of the XeO excimer *Appl. Phys. Lett.* **85** 4869–71
[13] Eden J G, Park S-J, Ostrom N P and Chen K-F 2005 Recent advances in microcavity plasma devices and arrays: a versatile photonic platform *J. Phys. D: Appl. Phys.* **38** 1644–8
[14] Lu M, Park S-J, Cunningham B T and Eden J G 2008 Low temperature plasma channels generated in microcavity trenches with widths of 20–150 μm and aspect ratios as large as 104:1 *Appl. Phys. Lett.* **92** 101928
[15] Eden J G *et al* 2013 Plasma science and technology in the limit of the small: microcavity plasmas and emerging applications *IEEE Trans. Plasma Sci.* **41** 661–75
[16] Kulsreshath M K, Schwaederle L, Overzet L J, Lefaucheux P, Ladroue J, Tillocher T, Aubry O, Woytasik M, Schelcher G and Dussart R 2012 Study of dc micro-discharge arrays made in silicon using CMOS compatible technology *J. Phys. D: Appl. Phys.* **45** 285202
[17] Lindner P J, Bender E and Besser R S 2014 Failure analysis of novel microhollow cathode discharge microplasma reactors *Int. J. Hydrog. Energy* **39** 18084–91
[18] Sillerud C H, Schwindt P D D, Moorman M, Yee B T, Anderson J, Pfeifer N B, Hedberg E L and Manginell R P 2017 Characterization of chemical contaminants and their spectral properties from an atmospheric pressure ns-pulsed microdischarge in neon *Phys. Plasmas* **24** 33502
[19] Felix V, Lefaucheux P, Aubry O, Golda J, Schulz-von der Gathen V, Overzet L J and Dussart R 2016 Origin of microplasma instabilities during DC operation of silicon based microhollow cathode devices *Plasma Sources Sci. Technol.* **25** 25021
[20] Kulsreshath M K, Golda J, Felix V, Schulz-von der Gathen V and Dussart R 2014 Ignition dynamics of dry-etched vertical cavity single-hole microdischarge reactors in ac regime operating in noble gases *J. Phys. D: Appl. Phys.* **47** 335202
[21] Rousseau A and Aubert X 2006 Self-pulsing microplasma at medium pressure range in argon *J. Phys. D: Appl. Phys.* **39** 1619–22
[22] Aubert X, Bauville G, Guillon J, Lacour B, Puech V and Rousseau A 2007 Analysis of the self-pulsing operating mode of a microdischarge *Plasma Sources Sci. Technol.* **16** 23–32